Effective monitoring of reservoir-induced seismicity utilizing integrated surface and downhole seismic networks

Gisela Viegas,[1] Adam Baig,[1*] Wade Coulter[1] and Ted Urbancic[1] show how enhancing a seismic network with high-sensitivity low-frequency accelerometers make it possible to correctly extend the recording range from –Mw3 to +Mw3 and properly assess the behaviour of reservoir-induced seismicity.

Many injection processes are monitored through the use of microseismic monitoring at short distances by the detection and analysis of micro-earthquakes. Hydraulic fracturing and cyclic steaming are capable of generating thousands of micro-earthquakes with magnitudes typically ranging from –Mw4 to –Mw1. The instrumentation and configuration of the microseismic monitoring networks are chosen with this magnitude range in mind, and the relatively high frequency signals are recorded with geophones with the bandwidth necessary for accurate spectral characterization. Also, the recording parameters typically trigger only short-time windows once an event has been detected. While these parameters may be acceptable for the characterization of such small magnitude events, they are not ideal for the characterization of larger magnitude events with Mw>0 to approximately Mw3 because the lower frequency signals emitted by these events will not faithfully be recorded and the pre-set time windows are too short to contain both P and S arrivals.

In our paper, we describe how the use of a hybrid surface-downhole array with both high-frequency and lower-frequency sensors can overcome these limitations by examining seismicity generated during a water flood injection programme in a hydrocarbon reservoir. While the majority of the events detected have moment magnitudes between –Mw2 to Mw0, there are a few Mw2 macro-events that were detected and felt at the surface. Since such larger magnitude events are relatively uncommon, it is critical to understand their behavior and accurately obtain estimates of magnitude for any risk and hazard assessments. Because the installed network incorporated surface-deployed, force-balanced accelerometers (FBAs) with longer-period recording, we not only were able to accurately characterize events in the more conventional microseismic magnitude range as detected on the downhole geophone arrays, but also characterize the larger events that occurred as a result of reservoir injection activities thereby improving the overall reservoir management system.

Hybrid seismic network

The seismic monitoring network is comprised of surface and downhole components. The downhole component of the seismic monitoring network consists of eight-level arrays of 4.5 Hz three-component component geophones close to surface (within 150 m) and 15 Hz three-component omni-directional geophones deployed deeper, in 11 vertical downhole observation wells. Additionally, a network of five surface-deployed, force-balanced accelerometers augment the downhole array, two of which are collocated with observation wells.

Considering both the downhole and surface networks, the approximate total areal extent of this array is approximately 150 km^2 (12.7 km x 12.2 km). When a sensor is triggered, the recording windows are a function of the type of sensor: for the 15 Hz and 4.5 Hz geophones this window is 6.5 sec long while the accelerometers employ window lengths from 1 min to 5 min, depending on the separation between the P and the S waves. These longer windows ensure that the waveforms from more distant events are captured. Events located in the reservoir will have total location accuracy from around 50 m to 100 m, although when events are detected on certain combinations of arrays, event locations become more accurate, with typical errors of 30 m or less.

Instrumentation

Geophones are passive mechanical velocity sensing devices based on a mass-spring system where, inherently, they can only measure movement of the reference mass. In the absence of movement the geophone reference mass remains at rest and therefore cannot provide any signal relating to the physical orientation of the device. A geophone's ability to detect low frequencies is governed by the physics of a mass-spring system and typically requires physically larger devices to detect increasingly lower frequencies. A similar limitation exists for specific types of accelerometers (e.g., a piezo-electric based accelerometer only outputs charge relative to the changing compression of the crystal).

[1] *ESG Solutions, 20 Hyperion Court, Kingston, Ontario, K7K 4R2, Canada.*
[*] *Corresponding author, E-mail: adam.baig@esgsolutions.com*

An enhancement to lower frequency detection from a physically small device is to measure the force it takes to hold the mass still. A further enhancement is to ensure that the mass is held in its centre position, referred to as force balancing. There are a variety of force-balanced technologies available ranging from enhanced geophone performance at low frequencies to MEMS (micro-electronic mechanical machines) accelerometers capable of measuring the static force of gravity. In the latter case, the effort taken to keep the reference device centred is proportional to the gravitational vector. The final selection of an appropriate device for low-frequency detection depends on factors ranging from physical size to expected reliability when installed.

The FBA type sensors utilized in this study have a flat response from 0 Hz to the Nyquist frequency. Active electronic devices inherently add their own noise signature to the system; often the noise signature is more significant at lower frequencies (referred to as 1/f noise). To ensure that the electronic components did not raise the noise-floor and that the signals of interest could be detected, a low frequency limit on the FBA was imposed through the digitizer (0.7Hz). Installation of the FBAs was on cement platforms in buried vaults at surface. Noise levels were determined for individual sensor axes and sensors were oriented in the local reservoir coordinate system.

Geophones are quieter than FBAs because they do not generate electronic noise, but as frequency increases the advantage of the geophone is lost because velocity rolls off from velocity at 20 dB per decade. However, in the frequency band of interest for microseismic events, typically with dominant frequencies up to 300 Hz – 500 Hz, geophone elements can faithfully reproduce incoming signals. In this study, all downhole geophone arrays were deployed on tubing and permanently installed by cementing. This ensured good coupling with the formation and low geologic operational noise levels.

All cabling and recorders were installed at distance from the sensors to minimize any electronic noise 'pick-up'. Solar power with batteries was used for both the surface and downhole instrumentation and data transmission was achieved through a local radio network to a central data collection and storage site. Continuous signals were recorded with distributed 24 bit data recorders at each network node location. Sampling was carried out at ¼ ms or 4 kHz for all data streams; however, signals from the FBAs were decimated to 1k Hz sampling rate thereby improving the dynamic range. All signals included GPS time stamps for timing accuracy and triggering was achieved with a simple long-term average to short term average approach.

Case study: large events in hydrocarbon reservoirs

Underlying the study area, there is a number of hydrocarbon-bearing layers: a sandstone and shale gas reservoir is overlying a carbonate oil reservoir. Above the oil-bearing layers where the water injection is taking place, there is ongoing gas production that has been driven by natural depletion resulting in a decrease in reservoir pressure since the onset of production over 20 years ago. As is frequently observed, the depletion of the reservoir is accompanied by surface subsidence resulting in the occasional felt earthquake. No records of felt-earthquakes existed prior to hydrocarbon production.

Over a period of 10 months, the hybrid surface downhole network monitored seismicity in and around the reservoir. In general, over the monitoring period, there are few events detected each month, however, on at least one occasion there were 100 events detected in a single month. The magnitudes for these events range from micro-earthquakes at about –Mw2 to regional earthquakes at of about Mw3. Of these events, however, less than 3% are greater than Mw1. The locations of this seismicity is largely along a conjugate set of pre-existing, high-angle normal faults in the reservoir that are relatively shallow, around 1 km deep, and well above the depth of the injection (2 km). These locations are consistent with the hypocentres determined in previous studies in the reservoir (e.g., Sarkar et al., 2008; Kuleli et al., 2009; Li et al., 2011), where events were also found to locate predominately in the gas reservoir on pre-existing faults.

From these earlier studies, a good correlation was found between gas production and micro-seismicity, leading Sarkar et al. (2008) to suggest from the seismicity observed between 1999 and 2007 that the depletion and subsequent compaction of the reservoir is the primary cause for the events with relatively few events induced by the injection of the water. They concluded that the reactivation of the large-scale fault is the manifestation of this depletion and compaction.

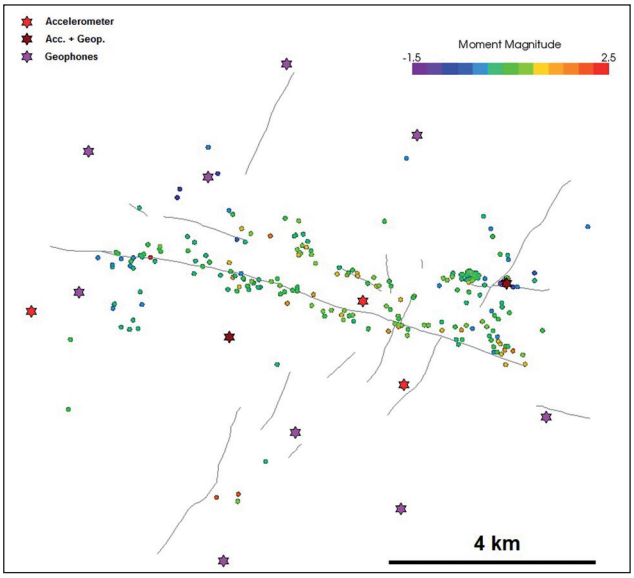

Figure 1 *Seismicity and seismic network map. The starts show the location of the observation wells and surface stations. The micro-earthquakes (circles) are colour-coded by magnitude and the grey lines represent regional faults.*

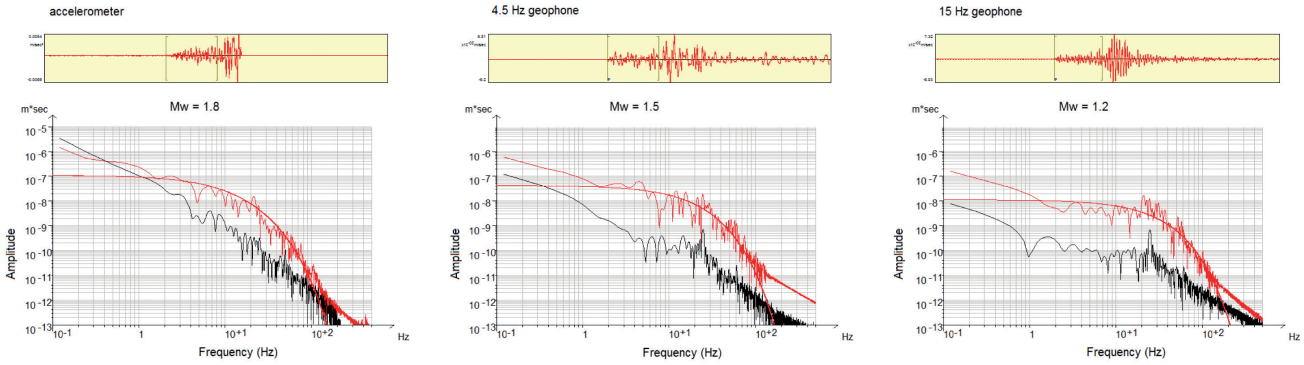

Figure 2 *Spectral modelling of SH waves recorded at three different sensors: (left) accelerometer; (middle) 4.5 Hz geophone and; (right) 15 Hz geophone. Using geophone data alone underestimates the moment magnitude estimates of this Mw1.8 event. Accelerometer data gives the correct Mw. Q is held constant in the Mw calculations.*

The smaller events, between –Mw1 to Mw1, from the same time period were analyzed by Li et al. (2011) who determined from moment tensor inversion that most of the events have a strike direction that is parallel with these major faults, also consistent with the hypothesis of fault reactivation. The majority of these mechanisms were normal faulting, leading Li et al. to suggest that, in the reservoir, vertical stress is larger than horizontal stress.

The dataset that we consider consisted of around 400 reservoir induced micro-earthquakes, observed between June 2011 and March 2012. For the purposes of this study, the dataset was composed of 160 events (shown in Figure 1), which had good signal-to-noise (>3) on all three types of sensors comprising the network. This decimated dataset includes all the large magnitude events (Mw>2) but excludes many of the small magnitude events that do not have sufficient signal levels on the surface FBAs.

Moment magnitude

Moment magnitude (Mw) is a parameter that involves characterization of the low-frequency spectrum of the seismic or microseismic event. Often, when calculating the moment magnitudes over a large network of stations, the estimates from each station are averaged together, with some weights that can be applied to account for the instrument type or a number of other factors (e.g., attenuation). However, to fully examine how the heterogeneous sensor distribution is beneficial, we do not average the magnitudes in this fashion, but rather account for each instrument type separately. Hanks and Kanamori (1979) stipulate how to calculate moment magnitude from seismic moment, which itself is measured from the long-period spectral amplitudes of the displacement spectrum (see also Baig and Urbancic, 2010, for an overview of these calculations as applied to microseismic data) corrected for focal mechanism, source and site conditions, and geometrical spreading (Brune, 1970). This low-frequency plateau is a feature of many source models (e.g., Brune, 1970; Boatwright, 1980) that characterize the spectrum by the long-period level, corner frequency, and attenuation quality factor. From these quantities assessed from the displacement spectrum, the source parameters like moment, energy, source radius, stress drop, etc. are calculated.

In Figure 2, we show an example fit of a Brune spectrum to one of the larger events we consider, with Mw=2.3. This example features the spectra of the P waves as seen on all three of the sensor types that we discuss: an FBA; a 4.5 Hz geophone; and a 15 Hz geophone. The sensors shown are all associated with the same observation well, with the 4.5 Hz and 15 Hz geophone deployed downhole and the FBA on the surface, proximal to the well. A constant attenuation factor is applied to all of the spectra, but the influence of Q is to attenuate the high frequencies preferentially and does not affect necessarily the estimates of the long-period plateau in this example. This figure illustrates how the short-period stations (the geophones) underestimate the moment magnitudes of this large event; only the FBA accurately recovers the magnitude of Mw1.8, the other stations show saturation around Mw=1.8 and Mw=0.8. This depletion of low frequencies in the geophone records can also be observed by the breakdown of the noise signal around the natural period of the instruments which is not observed at the FBA record.

In Figure 3, we present a comparison of the magnitudes of all of the 160 events in our sub-dataset, as calculated from each sensor type. There is a definite systematic bias toward lower magnitudes for the large events in the dataset (Mw1–Mw2) when only the shorter-period geophones are used in the calculation. There is a similar bias towards lower magnitudes when comparing the magnitudes determined from the 15 Hz geophones versus the 4.5 Hz geophones. The median values of the independent magnitude datasets capture the effect of these biases: 0.7 for the FBAs; 0.6 for the 4.5 Hz geophones; and 0.4 Hz for the 15 Hz geophones. This comparison of datasets highlights how it is necessary to accurately capture the long-period spectrum in order to avoid underestimating the magnitudes.

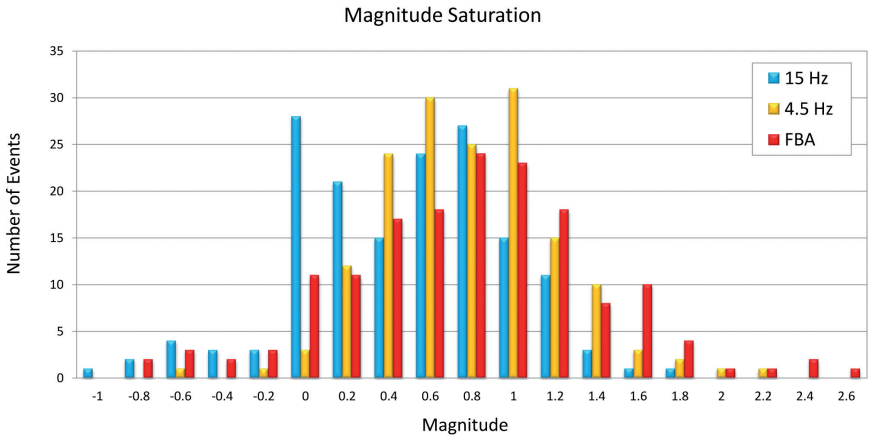

Figure 3 *Histogram with the distribution of event magnitude by instrumentation types for the same set of 160 events. Only force-balanced accelerometers (FBA) can accurately capture the magnitude of the larger events.*

Magnitude scale saturation

The effects observed in the previous section are well studied in the seismological literature, and the effect is known as magnitude saturation. Notably, this effect was observed for different magnitude estimates such as the m_b and M_S magnitude scales (see Hanks and Kanamori, 1979 and the references therein). As shown above, these effects can be understood in terms of the finite instrument bandwidth used to calculate the source parameters. For these scales, m_b is on the one hand determined from amplitudes of 1 s body waves, resulting in magnitude saturation at m_b6.0. M_S, on the other hand, is calculated from 20 s surface wave amplitudes, so it can more accurately determine large magnitudes but nevertheless is fully saturated around M_S8.0. In the example that we discuss, it is the natural frequency of the recording instrumentation that causes the calculated magnitudes to saturate.

To illustrate this effect, synthetic source spectra are computed from –Mw2 to Mw3 events in increments of half magnitude units. A constant stress drop of 0.1 MPa is used in these calculations, the median stress drop of the events estimated from the FBA data. For events with the same seismic moment, a higher stress drop event will have a higher corner frequency and vice-versa. The representation of the synthetic spectra computed with a higher stress drop in Figure 4 would be equivalent in displacing the spectra to the right along the x axis and to the left for a lower stress drop. Saturation of the magnitude scale occurs when the long-period spectral plateaus fall completely outside the recording bandwidth. In other words, when the event corner frequency is below the natural frequency of the instrument, then we will observe magnitude saturation. For the case study that we discuss, the magnitudes start to saturate at around Mw 0.5 for the 15 Hz geophone, around Mw1.5 for the 4.5 Hz geophones, and at about Mw3 for the FBA (considering these sensors are calibrated with a cut-off frequency of 0.7 Hz). The scale will be fully saturated at higher magnitudes. In practice, recording and analysis of data would occur below these saturation limits.

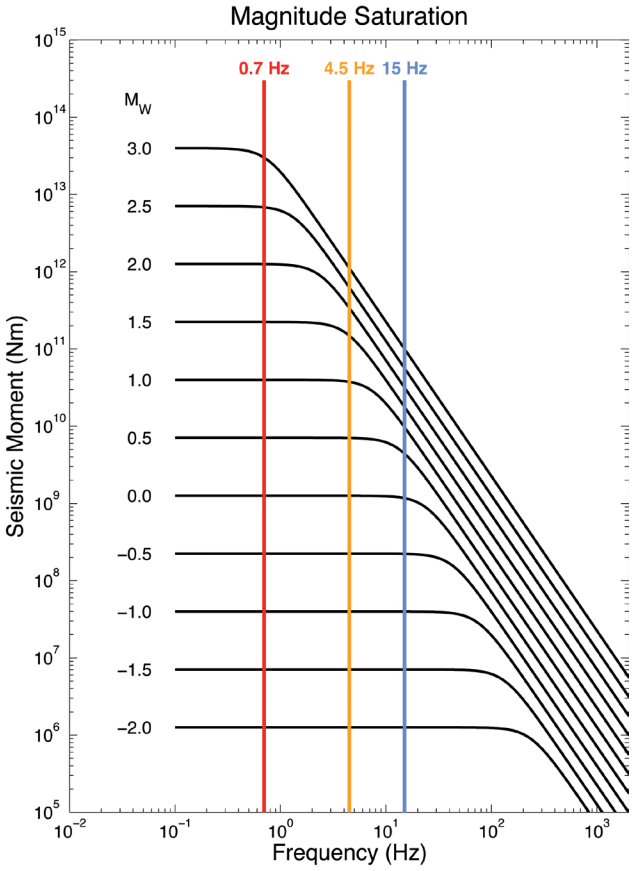

Figure 4 *Illustration of magnitude scale saturation for short-period instruments (15 Hz and 4.5 Hz geophones) for synthetic events with magnitudes comparable to the events recorded in the hydrocarbon reservoir. An average stress drop of 0.1 MPa was assumed for the synthetic spectra computation.*

The difference between the FBA-determined moment magnitudes and the magnitude estimates for each of the sensor types is shown in Figure 5. These residuals are mostly positive, highlighting how magnitudes are underestimated due to the scale saturation effects. Median values of the magnitude residuals are 0.2 comparing FBAs and 4.5 Hz geophones and 0.4 comparing the FBAs to the 15 Hz geophones.

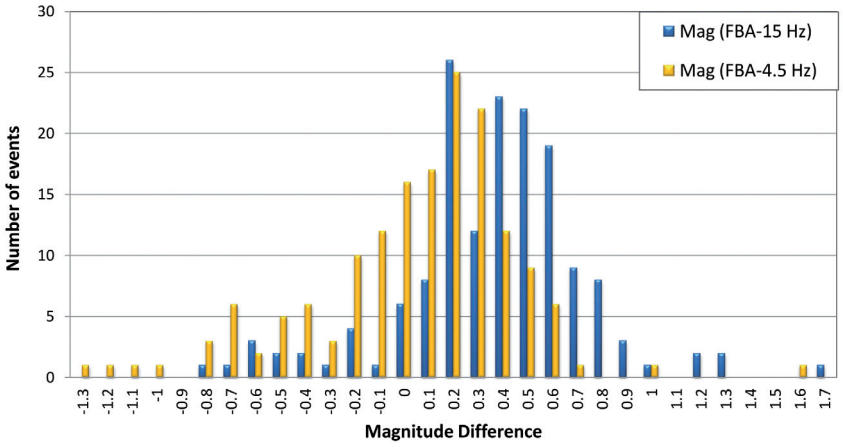

Figure 5 *Histogram showing the distribution of the differences between the obtained magnitudes using the FBA and each of the geophones.*

The effect is most evident for the largest magnitude events, as this is where the largest differences between FBA-determined and geophone-determined magnitudes exists. For these largest events in this dataset, only the FBA data will return accurate source parameters showing how these sensors are necessary to adequately characterize larger-magnitude, induced events.

Conclusions

A set of 160 events, with magnitudes ranging between Mw2 and Mw3 related to a water flood injection programme in a carbonate hydrocarbon reservoir at around 2 km depth are observed by a hybrid surface downhole array over a period of 10 months. Because this hybrid array consists of a heterogeneous distribution of FBAs deployed on the surface, and 4.5 Hz and 15 Hz geophones deployed downhole, the range of events in terms of moment magnitudes that can be accurately characterized is improved relative to an array of homogeneous sensors, because the hybrid system captures a fuller range of frequencies. Saturation of the moment magnitude scale occurs for events around Mw 0.5 for the 15 Hz geophones of Mw1.5 for the 4.5 Hz geophones, which are the typical instruments deployed for monitoring injections in these type of reservoirs. Only by including longer-period sensors, like FBAs, can the magnitudes of the larger events in this dataset be accurately calculated. Therefore, having these longer period instruments is essential for proper characterization of large events and avoiding magnitude saturation effects. Otherwise, the magnitudes of these large events will be under-estimated.

Most monitoring of injection-related microseismicity relies on 15 Hz geophones to characterize the source parameters (magnitude). We have shown that these sensors do not have the bandwidth necessary to accurately compute the size of earthquakes, when the corner frequencies of these events drop below the natural frequency of the sensor. The hybrid surface downhole array, with its complement of FBAs can recover the low-frequency signals necessary for proper characterization of these events, and their inclusion is essential for accurate characterization of larger-magnitude, injection- or stimulation-induced events. A hybrid configuration thereby increases the dynamic range of recordable signals from –Mw3 to +Mw3 and allows for the reduction of associated seismic hazards and risk associated with reservoir activities, and provides for effective reservoir design and management.

Acknowledgements

We would like to thank our colleagues at ESG for their support and in particular we would like to acknowledge Anisa Kassam and Margaret Seibel for their support in data analysis.

References

Baig, A. and Urbancic T. [2010] Magnitude Determination, Event Detectability, and Assessing the Effectiveness of Microseismic Monitoring Programs in Petroleum Applications. *CSEG Recorder*, **35**, 22–26.

Boatwright, J. [1980] A spectral theory for circular seismic sources: simple estimates of source duration, dynamic stress drop, and radiated energy. *Bulletin of the Seismological Society of America*, **70**, 1–28.

Brune, J. [1970] Tectonic stress and seismic shear waves from earthquakes. *Journal of Geophysical Research*, **75**, 4997–5009.

Hanks, T. and Kanamori H. [1979]. A Moment Magnitude Scale. *Journal of Geophysical Research*, **84** (B5), 2348–2350.

Kuleli, H. S.; Sarkar, S., Toksoz, M. N., Al-Kindy, F., El Hussain, I. W. and Al-Hashmi, S. [2009] Monitoring Induced Seismicity at an Oil/Gas Field, *American Geophysical Union, Fall Meeting 2009*, Abstract S31E-03.

Li, J., Zhang, H., Kuleli, H. and Toksoz, N. [2011] Focal Mechanism Determination Using High Frequency Waveform Matching and Its Application to Small Magnitude Induced Earthquakes. *Geophysical Journal International*, **184**(3), 1261–1274.

Sarkar, S., Toksöz, N., Kuleli, S., Zhang, H., Al-Kindy, F., Ibi, O., Al-Touqi, N. and Lewandowski H. J. [2008] Reservoir Monitoring Using Induced Seismicity: A Case Study from Oman, *EAGE Workshop*, Cyprus.